SUPPLEMENTARY INFORMATION

Supplementary Notes: The dynamics of measles in sub-Saharan Africa

Authors: Matthew J. Ferrari, Rebecca F. Grais, Nita Bharti, Andrew J. K. Conlan, Ottar N. Bjørnstad, Lara J. Wolfson, Philippe J. Guerrin, Ali Djibo, Bryan T. Grenfell

Contents

Appendix A: Critical community size for Niamey.

The critical community size (CCS), the population size necessary for long-term local persistence, for measles has been classically estimated at between 300-500 thousand[1,2]. We investigated the critical community size for Niamey by simulating realizations of the stochastic TSIR model with the estimated seasonality for Niamey and a low rate of stochastic immigration (10 infectious immigrants per year) as in Grenfell et al. [3]. We assumed the current birthrate for Niger (50.73 births per 1000 per year), discounted by a 70% vaccination rate. We simulated measles time series for 100 years, after a 100-year burn-in to account for transient dynamics. We then calculated the proportion of years with 0 fadeouts (2 consecutive bi-weeks with 0 cases) for communities ranging from 10 000 to 5 million. For comparison we also show the relationship between fadeouts and community size using the same model structure but with weaker seasonality consistent with that estimated for pre-vaccination London[2]. The strong seasonality in Niamey results in a CCS that is much greater than we would expect based on the classic assumptions for the industrialized world (Fig. S1) [1,2]. While the same model with London-type seasonality show very few fadeouts above 300-500 thousand, Niamey still shows significant fadeouts at populations of 5-10 million, which suggests that the long-term dynamics will continue to be highly erratic even as the city grows.

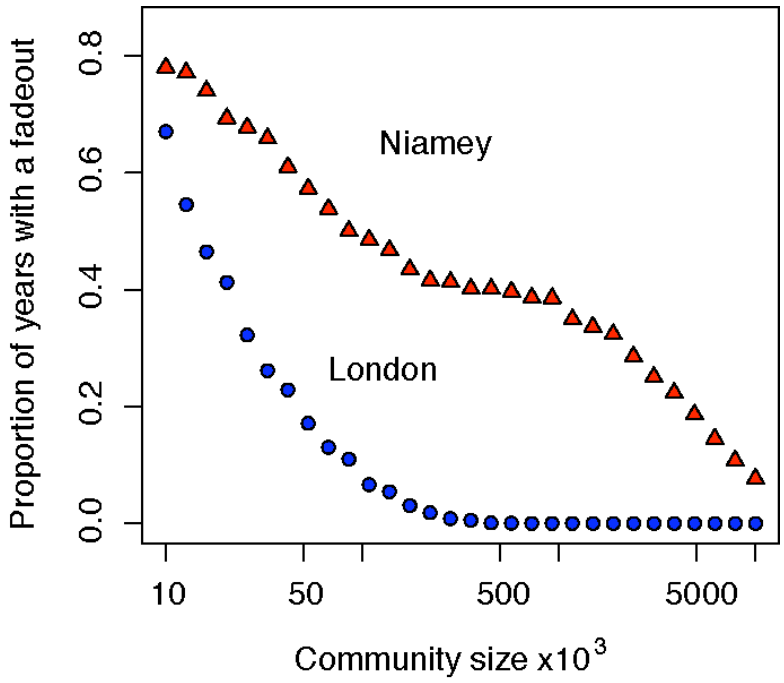

Figure S1. Critical community size for Niamey and pre-vaccination London. The y-axis indicates the proportion of years (out of 24) for which measles goes locally extinct (defined as 2 biweeks with 0 reporting). Red triangles give the mean proportion for 100 stochastic realizations of the TSIR model with the estimated Niamey seasonality and the observed Niamey birthrate with 70% vaccine coverage. The blue circles show the same for the pre-vaccination London seasonality with the observed birthrate.

Appendix B: Outbreak Detection

A key question in the face of erratic dynamics is how to optimize the decision to commit limited resources to ORV in a timely manner. The strong seasonality in Niamey works in our favour here, since surveillance may be enhanced when outbreaks are more likely. During the last 20 years, large outbreaks have tended to begin early relative to the seasonal fluctuation in transmission rate: 7 of 10 outbreaks of >2500 cases occurred when there were >10 cases reported in October, at the onset of the dry season (Fig. S2 vertical line). The seasonal nature of measles outbreaks in Niamey, and Niger as a whole, is familiar to regional public health workers and our quantitative analysis allows us to formalize this to develop a decision-rule for public health planning. For example, a possible action threshold for early response, which minimizes the likelihood of false positives, could be to initiate an ORV if the number of cases in October exceeds 10 (an 'October Rule') given the current level of vaccine coverage.

The 3 large outbreaks in Niamey that do not fit the 'October rule' followed years with <200 reported cases (Fig.S2 horizontal line). While the number of susceptibles is not directly observable, it relates inversely to the number of cases in the previous year [4]. Thus epidemic surveillance should be heightened both during the early dry season, when large outbreaks are likely to start, and if more than 1 year has passed since a major epidemic [5]. An action threshold could be a part of a larger vaccination and response program to minimize morbidity and mortality. If, following periods of low incidence, there is an indication of a potential outbreak, it may be necessary to consider vaccination even if the threshold level has not been met.

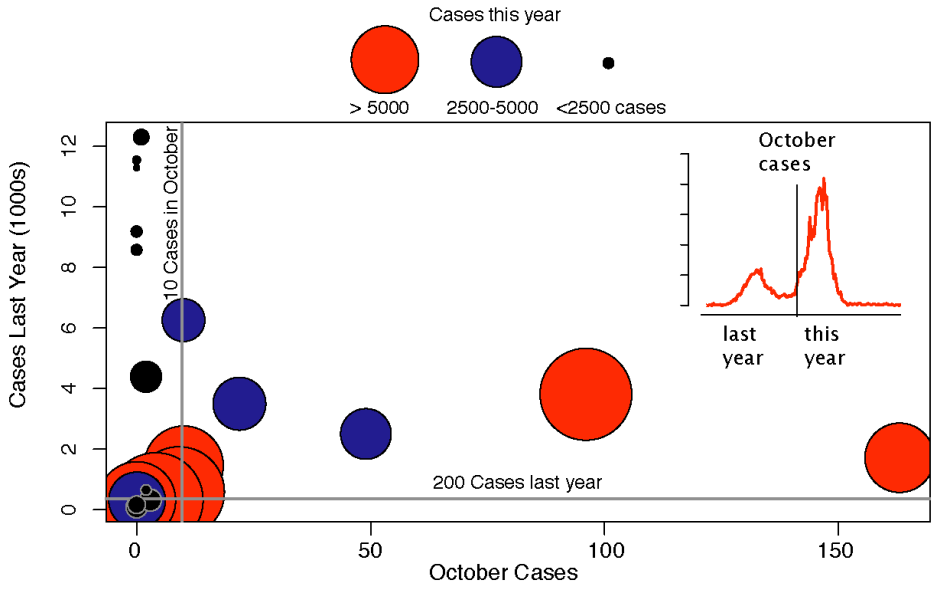

Figure S2. Monitoring for measles outbreak response
A) The number of measles cases in Niamey in the current year as a function of the number of cases in the previous year (y-axis) and the number of cases in October of the

current year (x-axis). The size and color of circles indicate outbreak size. Grey lines give the proposed thresholds for initiating a supplemental vaccination programme.

Recent interesting work by Stone et al. [6] has shown a relationship between the timing of epidemic peak and epidemic magnitude for moderately forced acute SIR dynamics. Based on their results we have examined the relationship between epidemic magnitude and epidemic peak for the Niamey measles time series from 1986-2005 (Fig. S3A and B) and for measles reports at the Arrondisement scale for 2001-2004 (Fig S3C) (2005 was left out as it followed an SIA). In both cases there is no clear negative relationship between the timing of the outbreak peak and the outbreak magnitude, contrary to the findings of Stone et al. The estimated seasonality in Niamey is much stronger than the forcing used in the Stone et al. simulations. Many of the outbreaks in Niger tend to be "curtailed" [6] by the decline in seasonal transmission rate prior to the exhaustion of the susceptible population. The result is that the timing of outbreak peaks in Niger tends to be strongly synchronous over a range of epidemic magnitudes (Fig. S3). As a result, peak timing has limited power to predict future outbreaks. Stone et al's work does, however, illustrate the potential of dynamical methods for measuring susceptibility during control programmes when the gold standard of longitudinal serology (e.g. [7]) is not available.

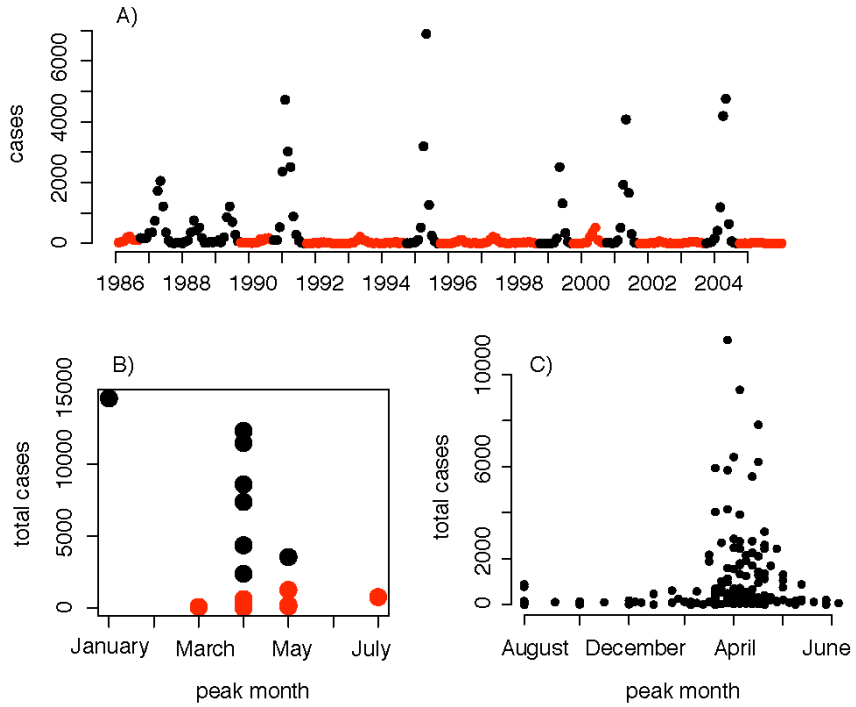

Figure S3. Relationship between the timing of epidemic peak and the epidemic size. A) The Niamey measles time series from 1986-2005, with small outbreaks and "skips" highlighted in red. B) The total measles epidemic size per year plotted against the month of the peak in cases for the Niamey time series from 1986-2005. Red indicates small outbreaks and "skips" as in A. Compare to Figure 1B,D in Stone et al. C) The total measles epidemic size per year plotted against the month of the peak in cases for 39 Arrondissements in Niger from 2001-2004.

Appendix C: Metapopulation model.

We studied the combination of routine and outbreak response vaccination (ORV) on the dynamics of measles outbreaks in a multipatch version of the TSIR model (Fig. S4). We simulated a spatially explicit metapopulation with population sizes and locations based on the 39Arrondissements of Niger plus Niamey (Figure S4A). Movement of infected individuals among communities was modeled as a commuter process with coupling strength that decayed as a power function of the distance between communities (Fig. S4B). Note that, exponential coupling could not replicate the observed dynamics. The coupling function requires two parameters; one to control the strength of coupling and one to control the rate of decay with distance. We fit the parameters by minimizing the sum of squares deviation between the observed spatial cross correlation among the communities from 2001-2005 (Figure S4C inset in main text) and that simulated by the metapopulation model. We chose this heuristic fitting approach[8] because the short spatially explicit time series. Lack of data also precluded us from fitting a full gravity model[8]. The distance decay parameter was well identified (Fig S5A), but a broad range of coupling strengths resulted in similar fit to the observed cross correlation (Fig S5B). To estimate the coupling strength we fixed the distance decay parameter at 1.7 and compared the predicted dynamics for Niamey over 1986-2002 (Fig S5C-E). We chose a coupling strength of 0.3, which resulted in realistic predictions for the observed outbreak frequency, persistence, and inter-annual variation for Niamey.

In the multi-patch setting, vaccination results in both an overall reduction in the average annual measles burden (see main text) and the rate of movement of re-colonization of communities following local extinction. This latter effect is particularly relevant in large, seasonal communities, such as Niamey, where measles tends to go locally extinct following the dry season. Thus, the reduction in overall number of cases leads to fewer infectious migrants and longer waiting times between re-introduction to communities from which measles has gone extinct. Consistent with expectation, increasing vaccination coverage, whether through routine vaccination or ORV, increased both the variability of the interval between large outbreaks in the Niamey (Fig. S6). The longer waiting times mean more time for the buildup of susceptibles and the potential for larger outbreaks upon reintroduction (see Fig. 3 in main text). This effect is compounded in highly seasonal settings, which naturally tend towards large episodic outbreaks, and recommends an increased role for monitoring outbreak response to mitigate the dramatic morbidity and mortality impact of such outbreaks.

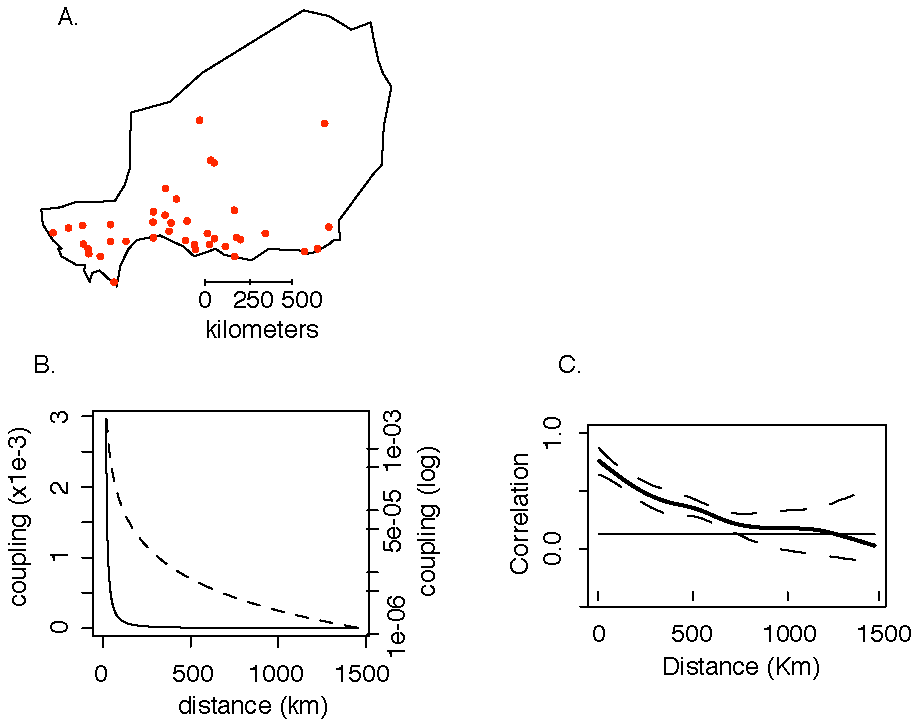

Figure S4. Niger regional metapopulation. A) Map of Niger with the major population centers of each of 39 the Arrondisements plus Niamey shows as red dots. B) Estimated coupling function for metapopulation model shown on arithmetic (left axis, solid line) and log (right axis, dotted line) scales. C) Correlation in Arrondissement time series as a function of distance. Dashed lines give 95% confidence limits.

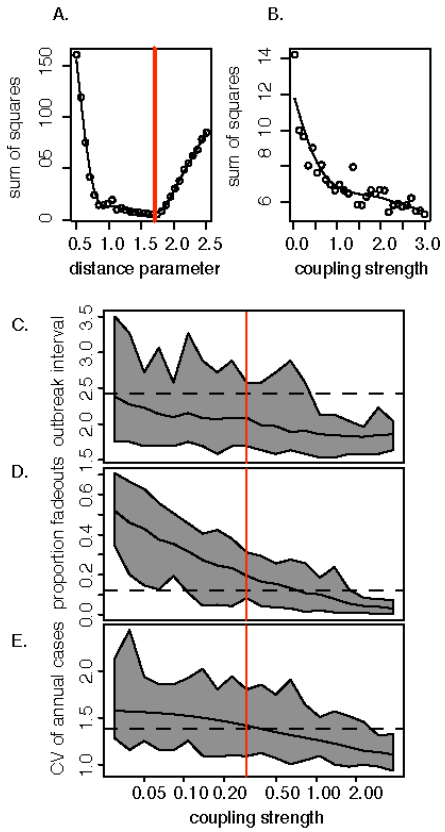

Figure S5. Parameter estimation or metapopulation coupling function.
A) Sum of squares fit between the observed (2001-2005) cross correlation function and that simulated from the metapopulation model as a function of the decay parameter. B) Same as A for the coupling strength. C) Predicted mean interval between large outbreaks in Niamey as a function of the coupling strength. Grey shading gives the range of outcomes from 50 simulations, solid black line gives the mean interval. Dashed line gives the observed interval for Niamey from 1986-2002. Red vertical line indicates the coupling strength used in the model: 0.3. D) Predicted proportion of weeks with 0 cases (fadeouts) in Niamey as a function of the coupling strength. E) Predicted coefficient of variation (CV) in annual cases in Niamey as a function of coupling strength.

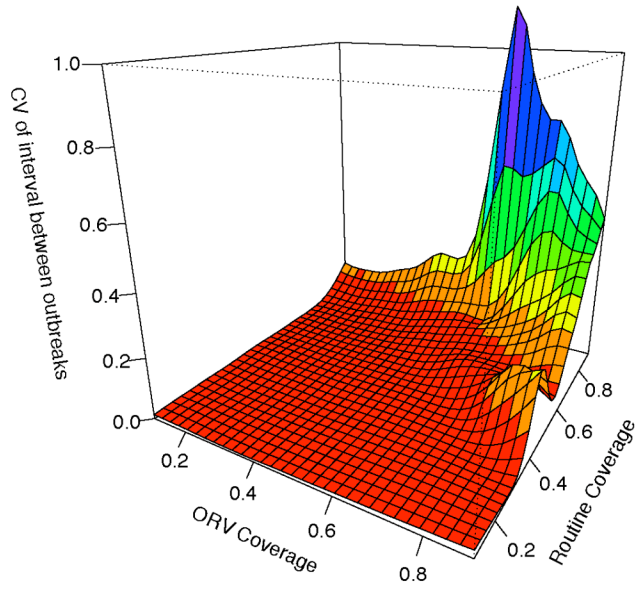

Figure S6. Coefficient of variation (CV) of the interval between large outbreaks (>2500 cases) in Niamey for a simple metapopulation model as a function of the routine (EPI) vaccine coverage and the ORV coverage. The mean is taken over 50 years of a stochastic simulation.

Appendix D: Sensitivity of metapopulation model to changes in reactive vaccination strategies.

Based on the metapopulation model described in the main text, we explored two additional vaccination response scenarios. In the first we assumed that that the minimum possible return interval for outbreak response vaccination (ORV) was 4 years in Niamey only. The effect of vaccination on the mean annual number of cases and the size of large outbreaks is qualitatively similar to that of the 2-year case shown in the main text (Fig. S7). Of note is that ORV has a smaller effect on the average number of cases as the return interval for intervention is longer than the average interval between large epidemics.

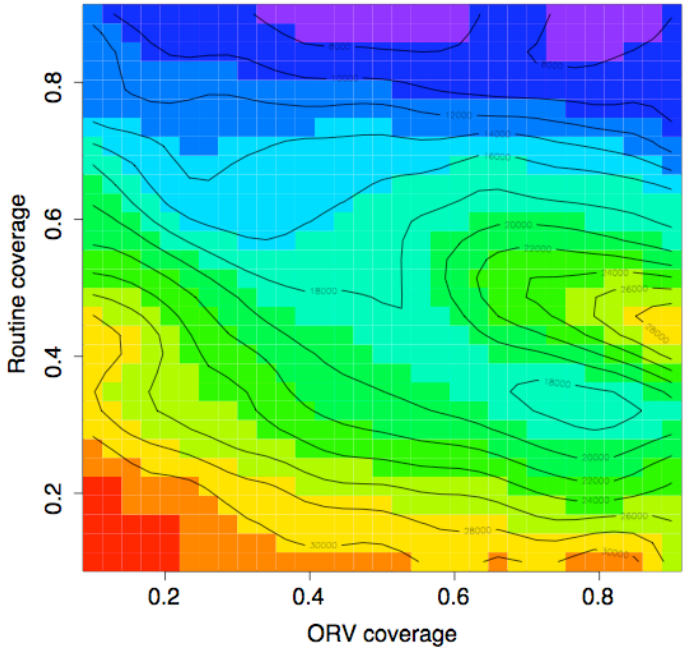

Figure S7. Outbreak size (colors and contours) in Niamey for a simple metapopulation model as a function of the routine vaccine coverage and the ORV coverage. ORV is limited to once every 4 years. The mean is taken over 50 years of a stochastic simulation.

In the second scenario, we applied ORV to the entire metapopulation (Fig. S8) with a minimum return interval of 2 years (as in the main text). As expected, the mean number of cases per year declines with increasing vaccination coverage (either routine coverage or ORV), however, it is striking that in this scenario, the size of large outbreaks is positively correlated with the ORV coverage when the routine coverage is lower than the herd immunity level (colored shading in Fig. S8). This counter-intuitive result occurs because ORV tends to stop outbreaks in the reservoir communities, reducing the

probability of re-introduction into Niamey. Thus, when routine vaccination is less than the herd immunity level, susceptibles tend to build up in Niamey allowing potentially larger outbreaks in non-ORV years.

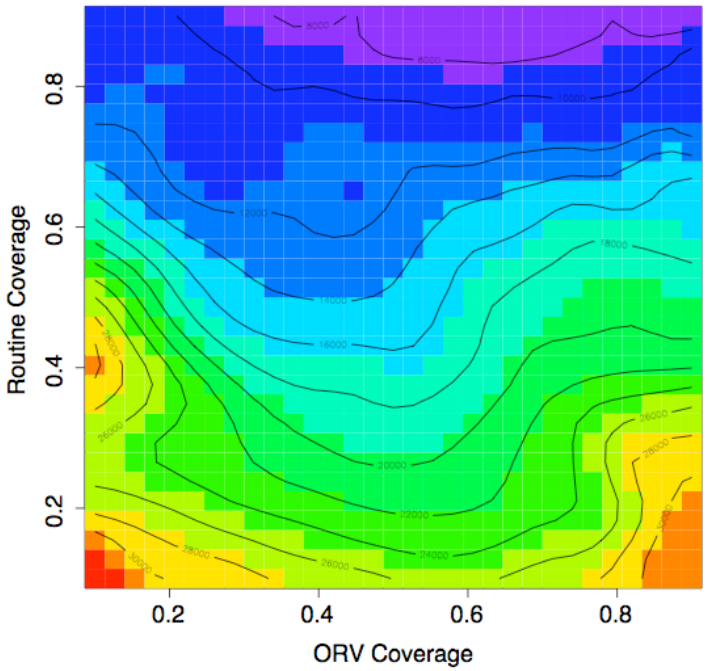

Figure S8. Outbreak size (colors and contours) in Niamey for a simple metapopulation model as a function of the routine vaccine coverage and the ORV coverage when ORV is applied to the entire metapopulation. The mean is taken over 50 years of a stochastic simulation.

Appendix E: Impacts of SIA vaccination

The measles vaccine, when delivered at 9 months of age, provides only 85% protection against infection [9]. This presents a significant barrier to achieving herd immunity in high-birthrate settings where opportunities for a second dose, necessary to achieve 99% efficacy, are often not routinely available. Thus, even with a relatively high level of routine single dose coverage among infants, there is still a significant recruitment of susceptible children into the population each year. The current SIA programme is designed to address this buildup of susceptibles due to imperfect routine coverage by providing a second dose to previously vaccinated children who have not developed immunity and a first dose to children missed by routine services. Our results for Niamey suggest that managing the build-up of susceptibility in non-outbreak years is key to interrupting the pattern of large, intermittent outbreaks. Catch-up campaigns such as the SIA programme appear to be key to this effort while the routine measles vaccination through EPI remains below the herd immunity level.

SIAs differ fundamentally from a reactive strategy in that the timing of vaccination is pre-determined. Such a strategy is, on one hand, more aggressive and can lead to greater levels of overall vaccination, though it is not as flexible in that there is no formal procedure to intervene with vaccination during outbreaks (i.e. ORV) that occur in non-SIA years. As SIA strategy in Niger has only recently been implemented, we are not able to do a formal analysis of its impacts based on observed time series. In lieu of a time series analysis, we investigated the effects of an SIA strategy through simulation on the seasonal multipatch model (Methods). We simulated epidemic dynamics in the multipatch model, as described above, with SIAs scheduled at 4-year intervals beginning on November 1 (the beginning of high seasonal transmission) with varying levels of vaccine coverage achieved in individual SIAs.

SIA strategies can be highly effective at reducing the average annual measles incidence (Fig S9A). Further, SIAs can impact the dynamics of occasional measles outbreaks (Fig. S9B). For a given level of routine coverage, increasing the vaccine coverage achieved during individual SIAs will tend to shift the average interval between measles outbreaks to the frequency of the SIAs. In our simulations, increasing the coverage achieved by an SIA tended to move the dynamics from large outbreaks approximately every 2 years (observed frequency in Niamey from 1986-2002 was 2.4 years) to large outbreaks approximately every 4 years (the scheduling interval for the SIAs; Figure S9B). Initially, increasing the coverage achieved during SIAs resulted in a decrease in the size of outbreaks. As the interval between outbreaks moved from 2 to 4 years there is more time for the susceptible population to build up. As a result, there is an increase in the average size of outbreaks over when the SIA coverage increases from 20 to 45%. Note that the average number of cases per year decreases over this time (Fig S9A). Above ~45% SIA coverage, however, the dynamics are locked on a 4 year frequency and both the average number of cases per year and the average size of large outbreaks declines Fig. S9B).

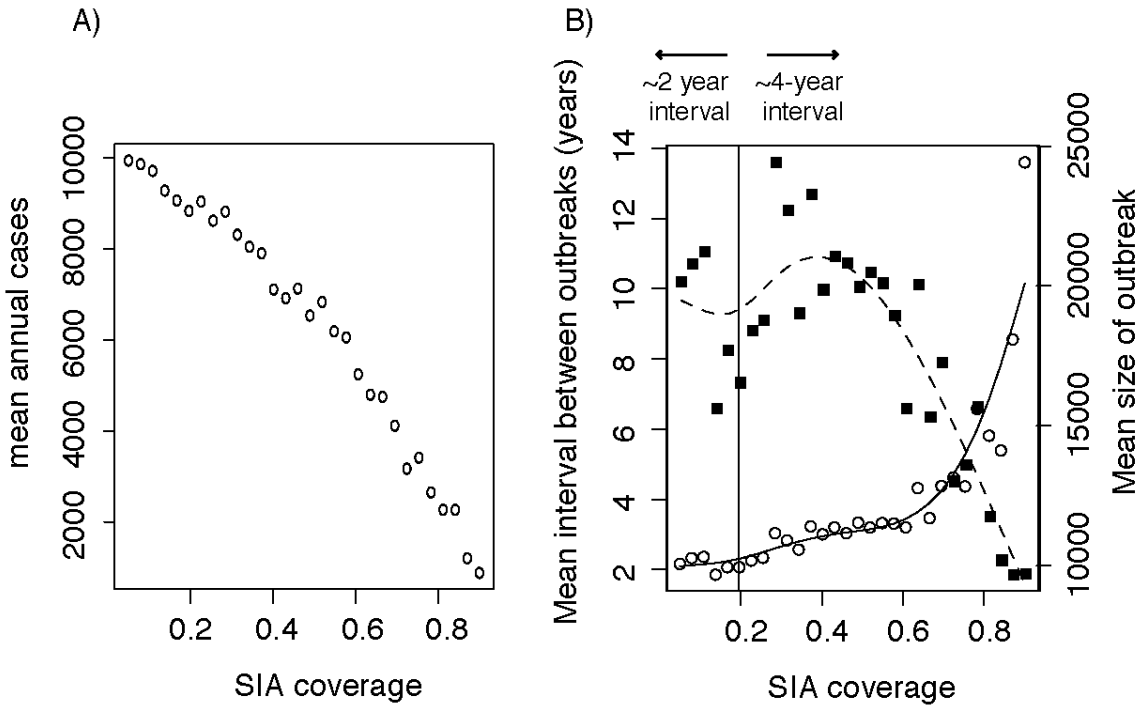

Figure S9. Simulated impact of SIA coverage on measles incidence in Niamey.
A) Mean annual cases, over 100 period, in Niamey under a 4-year SIA schedule plotted as a fuction of the coverage of the SIA. Routine vaccine coverage is assumed to be 75%.
B) Effects of SIA vaccination coverage on the mean periodicity (open circles, solid line) and magnitude (solid squares, dashed line) of large measles outbreaks.

Appendix F: Fitting the TSIR model

We estimated the seasonality for Niamey by fitting the time series of observed monthly cases to a time series SIR model [10] using a Bayesian state-space framework [11] to account for uncertainty in the observation. Following the standard assumptions for measles, we assumed the timescale for the unobserved epidemic process was approximately 2 weeks [10], which gives two unobserved epidemic time steps for each observed monthly report. Let Y_m be the reported number of cases in month m. These observed cases are assumed to be related to the unobserved number of cases each month, I_m, according to a binomial observation process with constant reporting rate, P_{obs}.

The unobserved epidemic process is assumed to follow the TSIR epidemic model [10]. Let I_t, be the true number of infected individuals at time step t, and S_t the true number of susceptible individuals. I_{t+1} depends stochastically on the number of infectious and susceptible hosts at time t with expectation $\lambda_t = \beta_m S_t I_t^{\alpha}$, where β_m is the month specific transmission rate and α is a parameter to account for non-linearities in transmission. Following the model of Bjørnstadt et al [12] we model I_{t+1} as a negative binomial random variable with expectation λ_t and clumping parameter I_t. New infections are drawn from the pool of susceptible individuals, which is, in turn, replenished by births. Thus, the number of susceptibles at time t is given by $S_{t+1}=S_t-I_{t+1}+B_t$, where B_t is the number of births. If we assume that the number of births is known from the nationally reported birth rate, then we can reconstruct the unobserved time series of susceptibles using the method described by Finkenstadt and Grenfell [10]. As there are no well reported data on time specific birth rates for Niger, we assumed that the birthrate was constant at 50.73 births per 1000 population per year [13], and that there was no seasonality in birth rates. We assumed that the effective birth rate into the susceptible class was discounted by the reported 70% vaccination rate. Further, this model assumes that the only fluctuation in susceptibles is the result of increases due to births and decreases due to infection. Thus, any seasonal fluctuation in the number of susceptibles due to rural-urban migration is not directly accounted for in the model, but will be reflected in seasonality in the time-specific transmission rates β_m. Human movements and seasonal migration may indeed play a strong role in seasonal transmission. In the absence of explicit data on movement, the transmission rate β_m is merely a proxy for perhaps very complicated fluctuations in mixing patterns and is an interesting area for future research. Additionally, if there is seasonality in the reporting rate, or if the reporting rate is a function of the incidence, this also will be reflected in the estimates of β_m leading to a potential bias in the estimated strength of seasonality. While this is a very real concern, we propose that bias due to incidence dependent reporting is minimal as the seasonal pattern of incidence is consistent in Niger across a range of population sizes (large and small towns) and across a range of outbreak magnitudes.

We fit the TSIR model using Bayesian state space framework, similar to that proposed by Morton and Finkestadt [11]. The susceptible reconstruction [10] provided initial estimates of the initial susceptible population size, S_0, and the observation probability. We chose a flat (uniform) prior for S_0 with the restriction that all $S_t > 0$ and chose a weakly informed prior for P_{obs} centered at the initial estimate from the susceptible reconstruction: *beta*(3.6,6.3). We initiated the chain with constant monthly transmission

rates, β_m, and used a beta prior with mean such that the effective reproductive ratio, R_E, was approximately 2: *beta*(0.8,1000). For the non-linearity term, α, we chose a beta prior that varied over the range 0.85-1.0: *beta*(100,5).

After a burn-in of 100 000 iterations, we ran the chain for 100 000 iterations sampled every 100th step to avoid auto-correlation. The predicted proportion susceptible varied between ~0.00 and 0.06 over the interval 1986-2002 (Figure S10). Note that the number of susceptibles drops to a very low level in 1991, near 0%. While unusually low, this did follow several years of moderate outbreaks and one large epidemic and was estimated robustly across independent MCMC chains. Estimates for β_m are given in the main text (Figure 2B main text). The marginal posterior distributions for the P_{obs} and α are given in Figure S11. Point estimates for P_{obs} and α are taken as the mean of the posterior distribution: P_{obs}=0.48 and α=0.98 respectively.

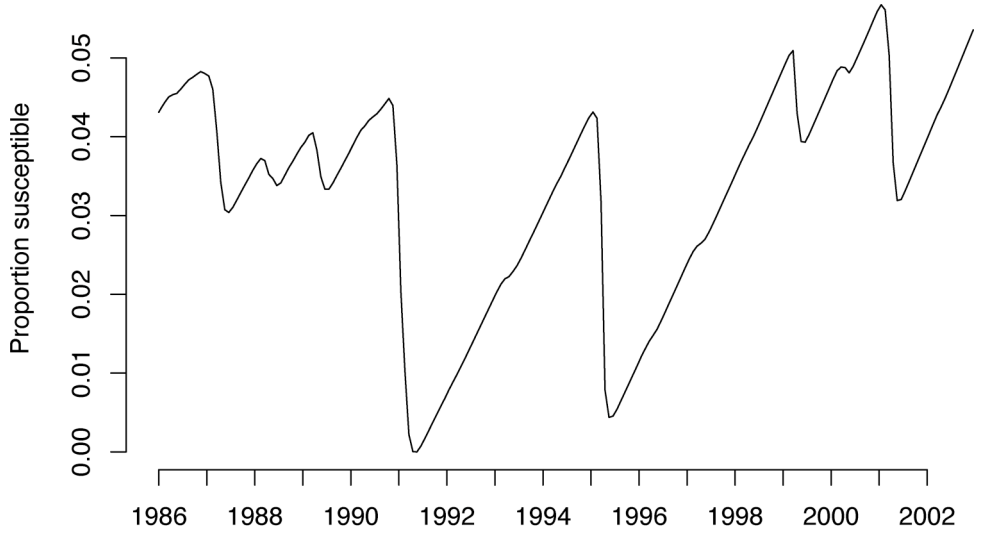

Figure S10. Predicted proportion of the population of Niamey that was susceptible to measles over the time period 1986-2002.

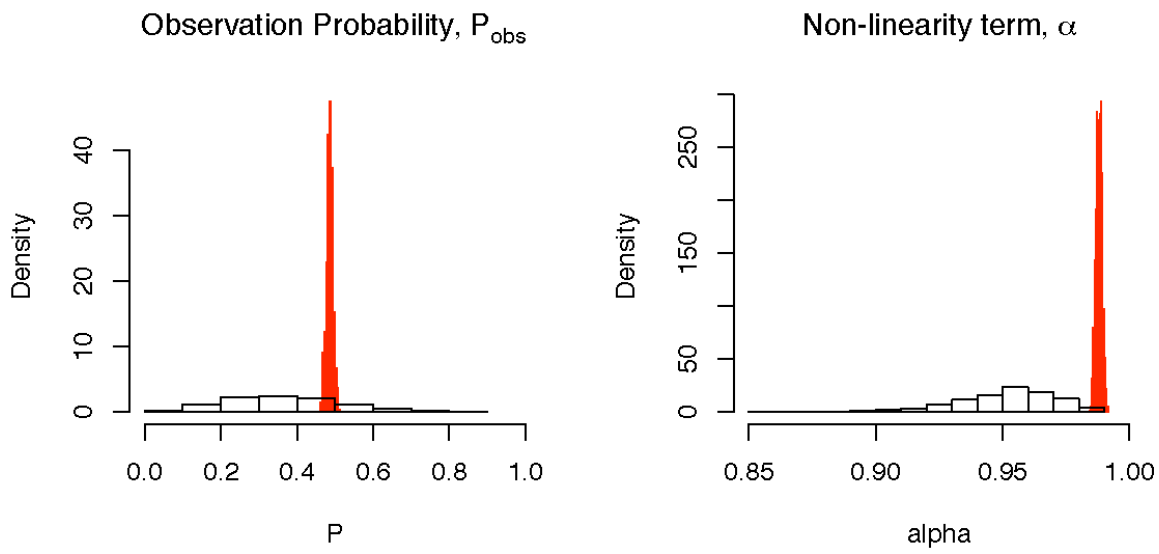

Figure S11. Prior and posterior distributions for the obserervation probability, P_{obs} (left), and non-linearity term, α (right). Prior distributions are given by the white histograms, posterior distributions are given by the red histograms.

References:

1 Bartlett, M. S., Measles Periodicity and Community Size. *J. R. Stat. Soc. A* **120**, 48-70 (1957).

2 Keeling, M. J. & Grenfell, B. T., Disease extinction and community size: Modeling the persistence of measles. *Science* **275**, 65-67 (1997).

3 Grenfell, B. T., Bjornstad, O. N., & Finkenstadt, B. F., Dynamics of measles epidemics: Scaling noise, determinism, and predictability with the TSIR model. *Ecol. Monogr.* **72**, 185-202 (2002).

4 Finkenstadt, B., Keeling, M., & Grenfell, B., Patterns of density dependence in measles dynamics. *Proc. R. Soc. Lon. B* **265**, 753-762 (1998).

5 Organization, World Health, WHO guidelines for epidemic preparedness and response to measles outbreaks, Available at http://www.who.int/csr/resources/publications/measles/WHO_CDS_CSR_ISR_99_1/en, (1999).

6 Stone, L., Olinky, R., & Huppert, A., Seasonal dynamics of recurrent epidemics. *Nature* **446**, 533-536 (2007).

7 Gay, N. J., Hesketh, L. M., Morgancapner, P., & Miller, E., Interpretation of Serological Surveillance Data for Measles Using Mathematical-Models - Implications for Vaccine Strategy. *Epidemiol. Infect.* **115**, 139-156 (1995).

8 Xia, Y. C., Bjornstad, O. N., & Grenfell, B. T., Measles metapopulation dynamics: A gravity model for epidemiological coupling and dynamics. *Am. Nat.* **164**, 267-281 (2004).

9 Wolfson, L. J. et al., Has the 2005 measles mortality reduction goal been achieved? A natural history modelling study. *Lancet* **369**, 191-200 (2007).

10 Finkenstadt, B. F. & Grenfell, B. T., Time series modelling of childhood diseases: a dynamical systems approach. *J. R. Stat. Soc. C* **49**, 187-205 (2000).

11 Morton, A. & Finkenstadt, B. F., Discrete time modelling of disease incidence time series by using Markov chain Monte Carlo methods. *J. R. Stat. Soc C* **54**, 575-594 (2005).

12 Bjørnstad, O. N., Finkenstadt, B. F., & Grenfell, B. T., Dynamics of measles epidemics: Estimating scaling of transmission rates using a Time series SIR model. *Ecol. Monogr.* **72**, 169-184 (2002).

13 CIA, World Factbook: Niger, Available at https://www.cia.gov/cia/publications/factbook/geos/ng.html, (2007).